

The System $\text{TiO}_2\text{-Cr}_2\text{O}_3$: Electron Microscopy of Solid Solutions and Crystallographic Shear Structures*

R. M. GIBB AND J. S. ANDERSON

Inorganic Chemistry Laboratory, University of Oxford, Oxford, England

Received August 6, 1971

The TiO_2 -rich end of the system $\text{TiO}_2\text{-CrO}_{1.5}$ has been studied by electron diffraction and electron microscopy, to examine the effects of controlled anion deficiency upon rutile-based structures. Materials equilibrated at 1330 K to 1570 K fall into three ranges. With > 15 mol % $\text{CrO}_{1.5}$, compounds of the known series $\text{Cr}_2\text{Ti}_{n-2}\text{O}_{2n-1}$, with (121) crystallographic shear planes are formed. With < 5 mol % $\text{CrO}_{1.5}$, rutile structure-defect solid solutions are found, with no shear planes. It appears that the anion deficiency is accommodated by point defects or small defect clusters. The limiting composition of this solid-solution range is strongly temperature dependent, and the rutile solid solutions are readily reduced, with the introduction of shear planes on (132), as for TiO_2 itself. Between these limiting ranges, well-ordered shear phases are formed, in which the slabs of rutile structure (the normal spacing between recurrent shear planes) remain constant but the orientation of the shear planes pivots round progressively from (121) to (132) as the anion : cation ratio is changed.

In spite of numerous investigations, the problems surrounding the ability of a given crystal structure to accommodate deviations from ideal stoichiometry have not yet been resolved. At the two extremes are those who discuss the problems in terms of classical point-defect theory and its elaboration to include interactions, and those who consider ordering effects, at least on a local scale, as dominating the structural consequences (1). Such ordering effects may include both superstructure ordering of vacant sites or of atoms on an interstitial sublattice and effects such as crystallographic shear which systematically eliminate sites from one sublattice.

Much recent work has been devoted to crystallographic shear structures, and particularly to the reduced rutile system TiO_{2-x} . The work of Magneli et al. (2-4) established that a series of discrete stoichiometric phases could be recognized in highly

reduced rutile, in the composition range $\text{TiO}_{1.75}\text{-TiO}_{1.90}$, conforming to the general formula $\text{Ti}_n\text{O}_{2n-1}$ ($4 \leq n \leq 10$), based structurally upon rutile and derived from it by regularly recurrent crystallographic shear. "Crystallographic shear" is used here in a topological rather than a mechanistic sense, and denotes the elimination of a complete set of anion sites from the parent structure, on some crystallographic plane (the crystallographic *shear plane*), with a mutual displacement of the two slabs of parent structure across this plane, defined in direction and magnitude by a crystallographic *shear vector*. This displacement or collapse preserves the octahedral coordination of the cations, but in the CS plane groups of $[\text{TiO}_6]$ octahedra in the rutile-based CS phases now share faces, and the coordination number of the oxide ions is thereby increased from 3 to 4.

The question is whether oxygen deficiency in rutile, arising either from chemical reduction in the binary system TiO_{2-x} or from the incorporation of cations of lower charge in ternary oxide solid solutions, can be fully accommodated by crystallographic shear without recourse to random, localized defects. In the composition range studied by Magneli, X-ray crystal-structure analysis defined the structural principle, and showed the CS plane

* Just as the manuscript of this paper was finished, an important paper was published by L. A. Bursill, B. G. Hyde and D. K. Philp [*Phil. Mag.* 23, 1501 (1971)] on the same subject. We debated whether to publish our own work, in the light of this prior publication, but concluded that the two investigations were in some respects complementary. Moreover, the concept of variable shear plane orientation is novel, and is strengthened by the fact that two independent groups have been forced to essentially the same interpretation.

to be {121} rutile with a shear vector close to $\frac{1}{2}\langle 0bc \rangle$. More recent work by electron microscopy and electron diffraction (5-11) has considerably amplified our knowledge. Direct lattice imaging has shown that the CS planes in oxides of the Magneli series are completely ordered and has revealed the existence of a second series of ordered phases $\text{Ti}_n\text{O}_{2n-1}$ ($\sim 16 \leq n \leq \sim 37$) in which the CS planes are {132} rutile. With increase in the oxygen:metal ratio, the spacing between successive CS planes increases (to about 4.0 nm at the upper end of the series) and several effects—the diminution in interaction forces and the small thermodynamic differences between compounds so closely spaced in composition—lead to loss of perfect long-range order. Direct lattice imaging reveals lamellae of different CS plane spacing (i.e., different members of the homologous series), fully coherently intergrown within small areas of crystal; the corresponding diffraction patterns reflect this 1-dimensional disorder by streaking of the superstructure reflections. Close to the stoichiometric composition ($x > 1.97$ in TiO_x), isolated faults are observed, lying in all the possible {132} rutile planes and randomly spaced. That these are CS planes has been established; Bursill and Hyde (8) were able to show from the fringe contrast at isolated boundaries that, as a result of the small distortions arising from face sharing between $[\text{TiO}_6]$ octahedra in the CS plane, the shear vector was $\frac{1}{2}\langle 0, 0.95b, 0.95c \rangle$ rather than a perfect lattice vector. Since numerous isolated {132}_{rutile} CS planes are already present in oxide of composition $\text{TiO}_{1.9986}$ (10), it might appear that point-defect anion vacancies or cation interstitials can be accommodated only in infinitesimal concentration in the rutile structure.

We describe here some electron-microscope observations on material in which the anion:cation ratio has been reduced by substitution of Cr^{3+} for Ti^{4+} . It is already known that the $\text{TiO}_2\text{-Cr}_2\text{O}_3$ system, in the range 12.5–20 mol % Cr_2O_3 , shows close similarities to the binary Ti–O system (2). A series of ordered phases is formed, isostructural with the Magneli binary oxides, and this based on regularly recurrent {121}_{rutile} CS planes, with the series formula $\text{Cr}_2\text{Ti}_{n-2}\text{O}_{2n-1}$ ($6 \leq n \leq 9$). The phase equilibria in this system at high temperatures have recently been discussed by Flörke and Lee (12); they consider the {121} CS phases to be “line” phases, of constant composition, which undergo a succession of disproportionation transformations as the temperature is reduced, whereby the lowest stable value of n in $\text{Cr}_2\text{Ti}_{n-2}\text{O}_{2n-1}$ increases from $n = 6$ above 1700 K to $n = 8$ at 1570 K. There is a homogeneous

solid-solution region, with an upper limit of about 7.5 mol % $\text{CrO}_{1.5}$ at 1570 K, the saturation limit decreasing with decrease in temperature; this is separated by a two-phase region from a range, which could not be elucidated by X-ray diffraction methods, but was considered to contain a series of ordered phases similar to those that have been identified in reduced rutile. The limiting $\text{CrO}_{1.5}$ content of this region was put at 14 mol % $\text{CrO}_{1.5}$ at 1570 K, moving towards lower $\text{CrO}_{1.5}$ content as the temperature is lowered. The tolerance of the rutile structure for oxygen deficient solid solution, whatever its constitution, diminishes at lower temperatures; the equilibrium range of intermediate phases appears at the same time to extend to phases of lower $\text{CrO}_{1.5}$ content, but the work of Flörke and Lee suggests that these phases are such that they involve progressively wider slabs of the TiO_2 structure. The work reported here bears particularly upon this part of the equilibrium system.

Experimental

Several samples were made with chromium contents between 2.0 and 25.0 at % $\text{CrO}_{1.5}$. Two methods were used for the preparations. For both methods “Specpure” titanium dioxide and chromium sesquioxide (Johnson and Matthey) were used. In the first method, the constituents were weighed out and then ground and mixed in an agate-ball mill before being pressed into a pellet. The pellet was then annealed in air at 1570 K in a “Crusilite”-element furnace for seven days. While in the furnace, the pellet was laid on a thin sheet of platinum in an alumina boat. The pellets were quenched by air cooling after being rapidly removed from the furnace.

In the second method, used for samples with low chromium content, the pellet was melted in an argon plasma arc for a few seconds, before being annealed. This was to ensure complete mixing of the chromium. The arc-melted pellet was annealed at 1570 K for fourteen days in air to allow the ordering processes to go on to completion. Equilibration at lower temperatures was achieved by subjecting the 1570 K materials to a second annealing process.

X-Ray powder diffraction patterns were taken of each sample using either a Debye–Scherrer or a Guinier–Hägg camera in order to identify the products.

The quenched samples were microcrystalline and appeared as dark grey, but on crushing, they took on a pale brown colour. Samples were prepared for

electron microscopy by crushing between two glass slides. The fragments were then deposited on a carbon coated grid.

Electron microscopy was carried out using a JEM 6A fitted with a goniometer stage with a tilt of $\pm 20^\circ$ and a 360° rotation, and on a JEM 100U fitted with a small angle tilting stage of $\pm 10^\circ$ and 360° rotation. The JEM 100U also has the facility for high-resolution dark-field microscopy in which the beam is tilted by means of electrostatic deflectors.

Results

The materials examined can be divided into three ranges, depending on the CrO_{1.5} content, and their general characteristics can be summarized as in Table I.

Range I: 0-5 mol % CrO_{1.5}

From the work of Flörke and Lee, these samples should lie within the composition range of a rutile solid solution. Electron diffraction showed that they were monophasic, with the rutile structure, and electron microscopy indicated that few defects were present, apart from dislocations and damage caused by fracture. A few crystal fragments contained thin lamellae which were identified as twins on {101} of the parent rutile structure. There is a considerable disparity in the size of the regions in the two orientations, and the widest twin lamellae observed were no more than 10 nm across. Within any given area of sample, the twins appeared on only one of the four equivalent {101} orientations.

No planar boundaries were observed within any fragment, as prepared and under normal operating conditions. If a fragment was beam heated, however, by removing the condenser aperture and slowly

focusing the beam, many faults were seen to grow across the crystal, extending along their length (Fig. 1).

In general two faults grew parallel to one another with only a small distance separating them. These pairs of faults frequently followed a zig-zag pattern, changing between two orientations. Not all the faults crossed the crystal from edge to edge, but some ended within the crystal and others when they intersected faults of another orientation. At A (Fig. 1), diffraction contrast shows a series of parallel faults at a regular spacing of 4 nm as determined from a microdensitometer trace. Further evidence for the fact that the faults occurred in pairs came from the observation that, in some orientations of the crystal, no contrast was observed in the centre of the fringe system as expected for planar faults inclined to the beam (13).

Since the fringe contrast was symmetrical in bright field, the isolated faults were identified as α -boundaries. In Fig. 1, faults in two different orientations are nearly parallel to the beam. In the corresponding and correctly oriented diffraction pattern, the streaking of the diffraction spots lies perpendicular to the faults and along the $\langle 132 \rangle$ direction of the rutile reciprocal lattice. The plane of the faults thus appears to be {132} and, on this basis, faults can be seen in this fragment along six of the possible {132} orientations. By using two-beam diffraction conditions, and observing the contrast at isolated faults for different diffraction conditions, the results agreed with those expected from a displacement vector close to $\frac{1}{2}\langle 0, b, c \rangle$ as observed for {132} faults in rutile (8). These faults are thus very similar to those observed in slightly reduced rutile and can be identified as crystallographic shear planes.

TABLE I

at. % CrO _{1.5}	1570 K	1420 K	1330 K
<5%	Isolated {132} CS only on beam heating and very low Cr content	—	—
7%	No boundaries	Close to {132} CS	Close to {132} CS
10%	CS along plane intermediate between {132} and {121}	—	—
15%	CS along plane intermediate between {132} and {121}	CS along plane intermediate between {132} and {121}	{121} CS

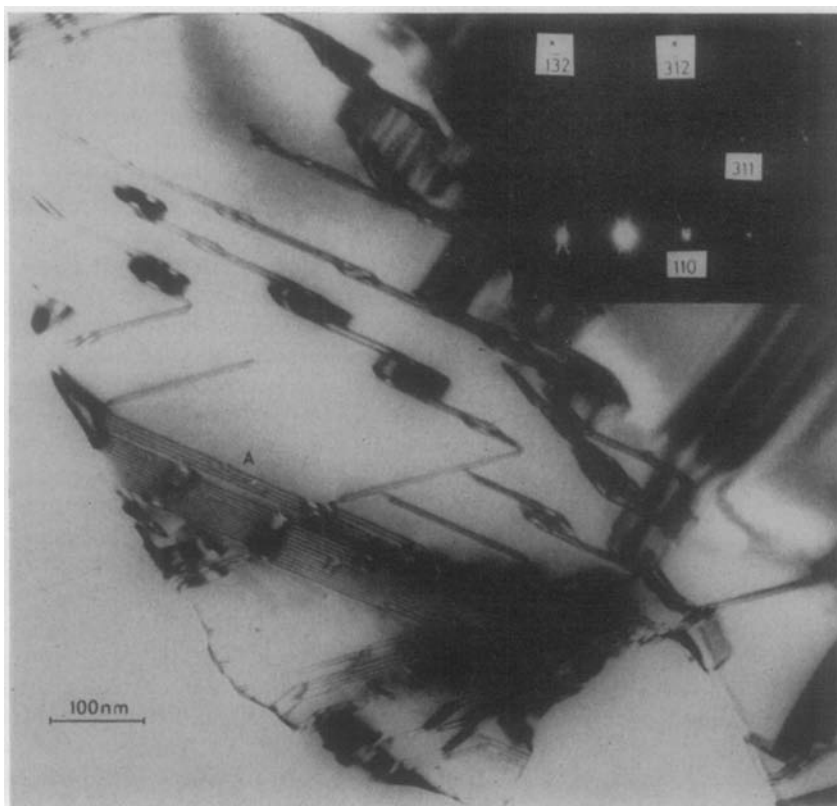


FIG. 1. Faults along {132} rutile in TiO_2 2% $\text{CrO}_{1.5}$ which formed after beam heating.

As stated above, no crystallographic shear planes were observed in the "as-annealed" samples in the composition range $\text{Cr}_{0.02}\text{Ti}_{0.98}\text{O}_{1.99}$ – $\text{Cr}_{0.05}\text{Ti}_{0.95}\text{O}_{1.975}$, and none was introduced into the latter material even by beam heating. It would therefore appear that there is a limited solid solution range in which Cr^{3+} can be introduced into the rutile structure without the formation of extended defects; formation of {132} CS planes during beam heating is probably to be interpreted as due to chemical reduction, as with rutile itself.

Range II: 15–15 mol % $\text{CrO}_{1.5}$

Up to approximately 10 mol % $\text{CrO}_{1.5}$, for samples annealed at 1570 K, the diffraction pattern was that of rutile. At about this composition, bands diffracting differently in bright field were observed (Fig. 2) and these were, in some cases, further subdivided into strips of differing contrast. By orienting the crystals to bring the boundaries edge-on to the beam, it could be shown that the strips were twinned with respect to the parent rutile structure, with the twin boundary lying along {100} and {001} in different crystal fragments, and with twin widths varying between 50 nm and 500 nm.

Further tilt brought the crystal into an orientation in which a series of weak superlattice spots could be observed. These were regularly spaced, although two different, superposed spacings along the same direction were found in some cases; the spots were slightly streaked. The direction of these arrays of superlattice reflections did *not* conform to a simple reciprocal-lattice vector of the rutile structure, but with some reciprocal-lattice sections it could be shown that the superlattice direction approximately bisected the $\langle 121 \rangle$ and $\langle 132 \rangle$ directions (Fig. 3).

Shear-plane spacings and perfection of ordering were examined by direct lattice imaging; with the specimen oriented to maximize the intensity of the superlattice spots, the main beam and four diffracted beams were combined by use of a suitable objective aperture. For many crystals, the lattice fringes could be observed only where they crossed a bend contour; this is a consequence of the low intensity of the superlattice reflections relative to the undeflected beam. It was therefore advantageous to form the lattice image in dark field, by combining the superlattice spots with one of the (much less intense) rutile diffracted beams, using the electrostatic beam tilting facility of the JEM 100U to bring

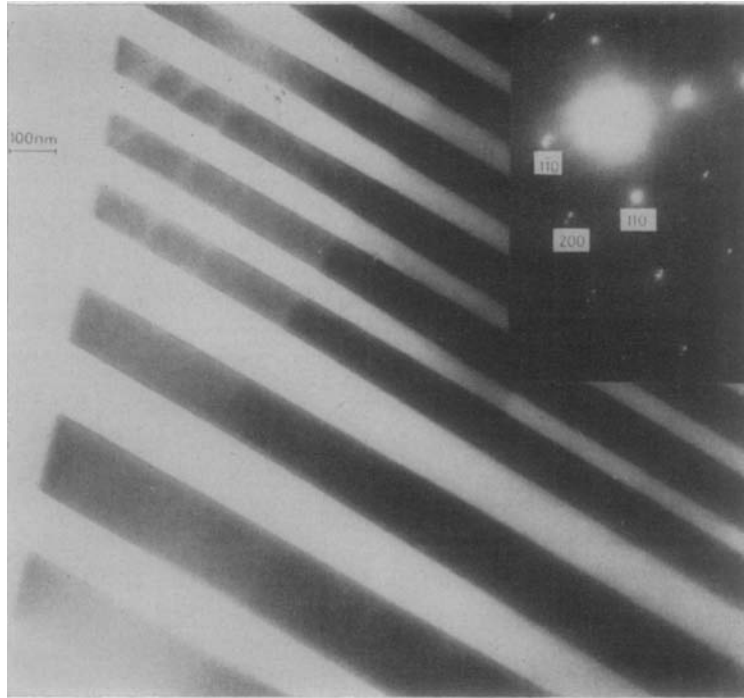


FIG. 2. Twin lamellae in a sample with approximately 5 mol % $\text{CrO}_{1.5}$ in which the twin boundary lies along (100) rutile.

the diffracted beams symmetrically through the centre of the lens system.

The superlattice repeat distance, as determined both from the diffraction patterns and from the resolved lattice fringes, covered a range of observed spacings between 2.07 and 2.25 nm. Fringe spacings

were measured from microdensitometer traces, which showed the ordering to be very regular over extensive areas of crystal. In some cases, lattice fringes could be resolved simultaneously from both orientations of the twinned structure (Fig. 4). The spacing (and by inference, the composition) in one

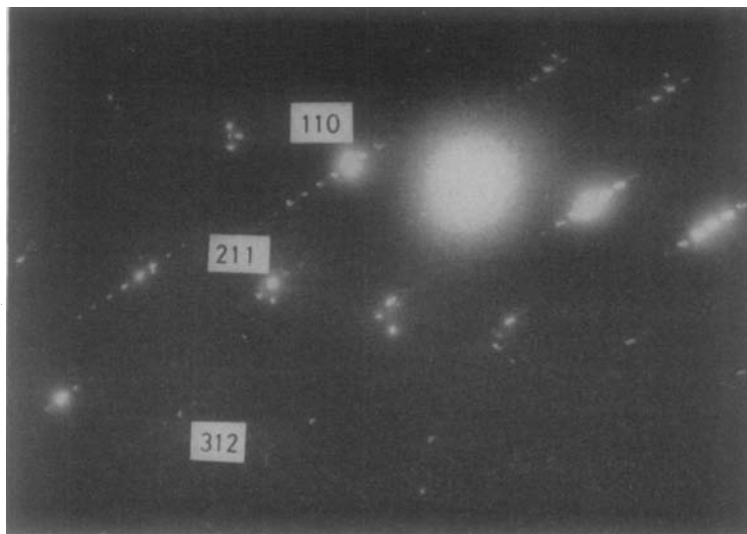


FIG. 3. Diffraction pattern showing superlattice direction bisecting the [211] and [312] rutile directions. The shear plane spacing from the diffraction pattern is 2.15 nm.

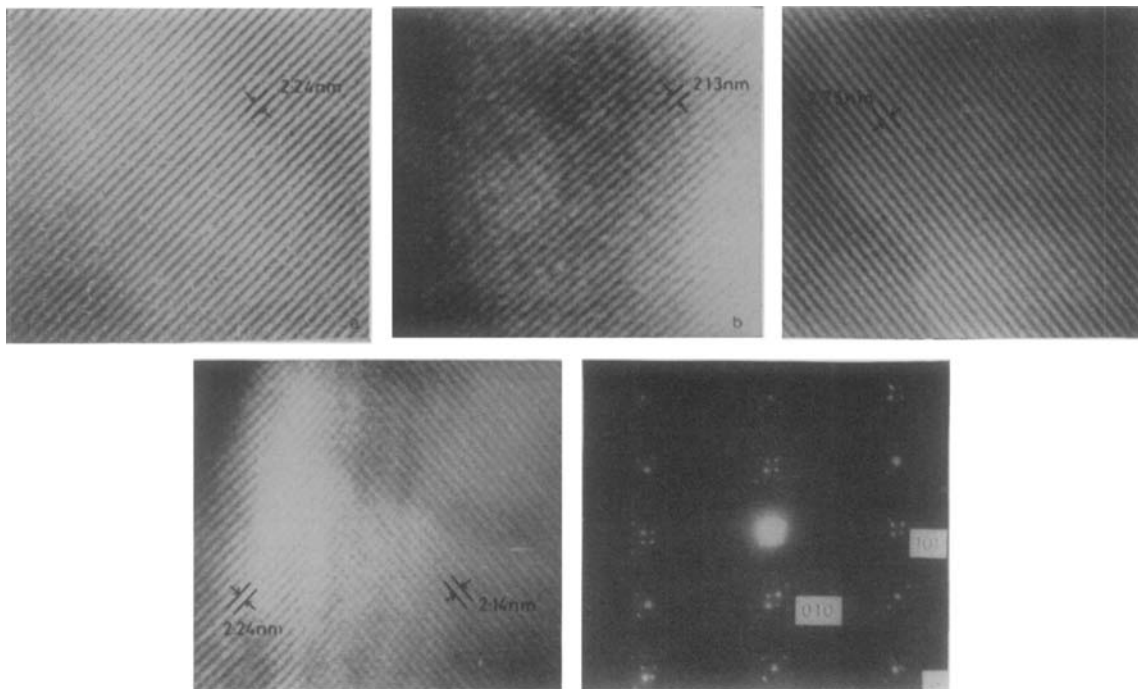


FIG. 4. Material twinned about (010) rutile. (a), (b) and (c) show fringes resolved from different twin lamellae using the 010 reflection. (d) shows resolved fringes at a twin boundary (the boundary is not parallel to the beam, hence the criss-cross pattern), (e) shows the relevant diffraction pattern.

twin orientation was not always the same as that in the other; “twinning” must therefore be used here in a special sense, implying the twinned orientation of the rutile subcell but not necessarily identity of superlattice structure. It was found, similarly, that twin domains of the same orientation did not necessarily contain superlattices of identical spacing and composition. Careful measurement of the angle between the CS plane fringes and the principal directions of the rutile structure indicated that, with differences in CS plane spacing, there were differences also in the orientation of the CS planes, which do not coincide exactly with either {132} or {121}.

Structural equilibration at lower temperatures gave somewhat different results: material with 13 mol % $\text{CrO}_{1.5}$ was reannealed at 1420 K and material with 7 mol % $\text{CrO}_{1.5}$ (which had shown no superlattice ordering as annealed at 1570 K) was annealed at 1330 K.

In the 13 mol % (1420 K) material, electron-diffraction patterns of two distinct types could be obtained from separate domains within the same crystalline fragment. The first had a superlattice spacing of 2.14 ± 0.03 nm, along a direction that could not be fixed exactly, but which lay between

[121] and [132]. The second had a superlattice along the [132] reciprocal lattice direction, with 27 spots between the origin and (132), corresponding to a superlattice spacing of 2.75 nm.

The 7 mol % (1330 K) was rather different. Some fragments had a superlattice of 2.75 nm close to the $\langle 132 \rangle$ directions, and some were observed to have the superlattice along $\langle 121 \rangle$; Fig. 5 shows a diffraction pattern of this type, from a crystal twinned about $(100)_{\text{rutile}}$, with a 14-fold superlattice along [211] equivalent to a spacing of 2.31 nm.

In other crystals, longer superlattices were observed, with spacings of 2.89 nm and 2.99 nm very close to [132]. When these were examined under high resolution, they were shown to be made up of lamellar domains, with superlattice fringes only in alternate domains (Fig. 6). There was no evidence of any diffraction spots from a second phase or from a twin orientation. The domain boundaries were not in the same plane as the CS planes of the superlattice lamellae, and it would appear that they do not correspond to a simple crystallographic plane. Indeed CS planes at the boundary appeared to terminate within the crystal, giving the boundary an apparently irrational orientation; there is some strain contrast about the

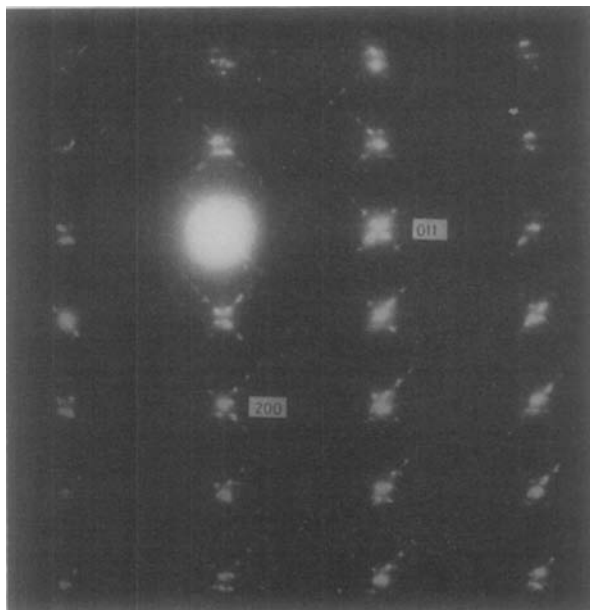


FIG. 5. Diffraction pattern from a fragment of $\text{Cr}_2\text{Ti}_{12}\text{O}_{27}$ which is twinned about the (100) plane.

termination of such CS plane fringes, which might be compatible with the postulate of a boundary dislocation loop (14). The conclusion is that crystal fragments of this type reveal an unmixing into domains of a rutile solid solution and domains of $\langle 132 \rangle$ CS phase, the latter having one or other of two compositions.

In a few cases, two different orientations of the CS phase lamellae could be observed within a single fragment. (Fig. 7); both components were of $\langle 132 \rangle$ type and such domains were of finite length, ending within the crystal.

Range III: 15–25 mol % $\text{CrO}_{1.5}$

In this range, the samples of higher $\text{CrO}_{1.5}$ content overlap the compositions of the shear phases identified by Magneli et al. The crystals showed twinning on $\{100\}$ and $\{001\}$ and displayed superlattice ordering. In most cases, the superlattice spots lay along $\langle 121 \rangle$ rutile, as is consistent with the earlier X-ray diffraction work, but in some cases the superlattice direction deviated by a small but significant amount from $\langle 121 \rangle$. Samples made up with compositions in this range gave lattice images, resolved in bright field, with the spacings shown in Table II, corresponding to n -fold superlattice multiplicities in the diffraction pattern, and compositions $\text{Cr}_2\text{Ti}_{n-2}\text{O}_{2n-1}$ with all integral n , $7 \leq n \leq 11$. As Fig. 8(a, b) shows, the structures are well ordered over extensive domains. The $7x$ superlattice was only observed in coexistence with the $8x$ superlattice [Fig. 8(c)]; both had the same orientation, with an abrupt discontinuity in the CS plane spacings at the boundary of coherent domains within the same macroscopic fragment of crystal.

Discussion

Chromium-doped rutile appears, from the observations recorded above to display some close analogies with the binary Ti–O system. It differs from the binary system in respect of the defect structure at low anion deficiencies, in the marked temperature effects on internal ordering equilibria and in the effects observed in an intermediate range of compositions.

At the higher chromium concentrations (>15 mol % $\text{CrO}_{1.5}$), the results are in accord with the existence of a homologous series $\text{Cr}_2\text{Ti}_{n-2}\text{O}_{2n-1}$,

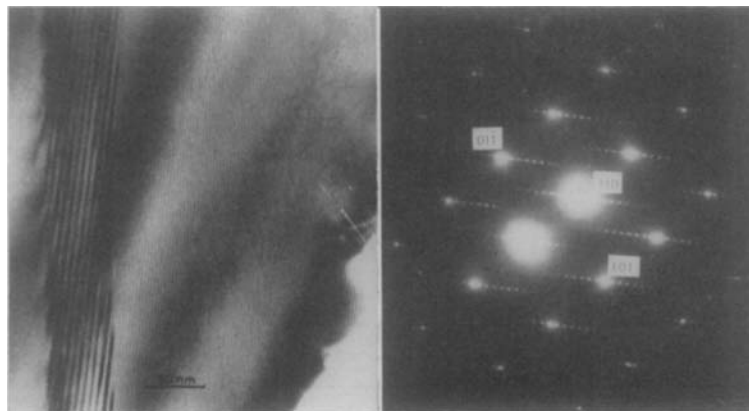


FIG. 6. Fringes resolved in a domain of $\text{Cr}_2\text{Ti}_6\text{O}_{11}$. Note the contrast at the domain boundary where the shear planes end in dislocations.

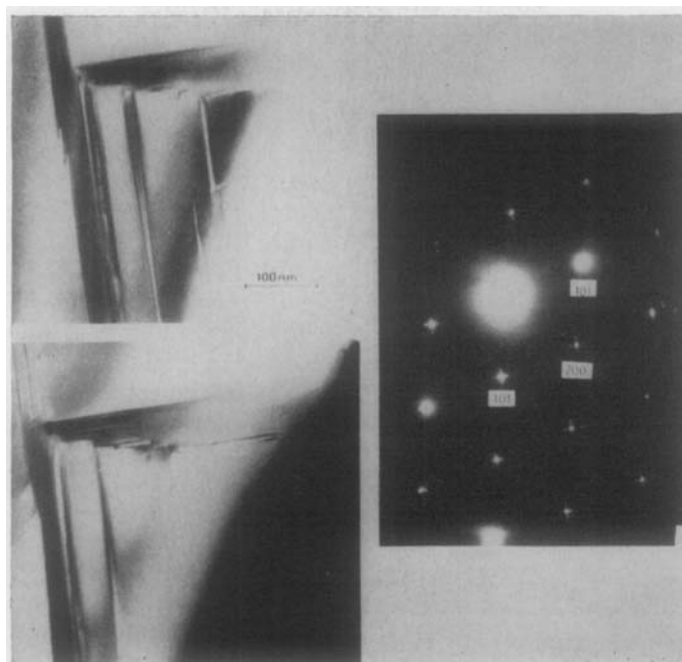


FIG. 7. Domains of ordered material on two equivalent orientations.

identified by earlier work (15) and the upper limit of this series appears to be $\text{Cr}_2\text{Ti}_9\text{O}_{21}$, $n = 11$. In the binary system, Hyde and Bursill find the upper limit of the $\{121\}$ CS plane series to be $\text{Ti}_{10}\text{O}_{19}$; the maximum spacing for ordering of $\{121\}$ CS planes is thus closely similar. The lowest member observed in this work was $\text{Cr}_2\text{Ti}_5\text{O}_{13}$, $n = 7$ (at 1570 K); this is not inconsistent with the phase diagram of Flörke and Lee, who give the lower disproportionation temperature of this phase as about 1600 K. Table II lists the observed $\{121\}$ CS phases, with the CS plane spacings as observed and as calculated

from the relation $D_{\text{CS}} = d_{121} (n - X)$, where the collapse factor X has been given the value $X = 0.347$ found by Bursill and Hyde (4).

At lower temperatures (1330 K, 1420 K) a second series of ordered phases was observed, which appear to be the analogues of the ordered $\{132\}$ CS phases of the Ti-O system. We could find only a few members of this family in preparations annealed at any temperature, and both the range of n and the maximum value of n in $\text{Cr}_2\text{Ti}_{n-2}\text{O}_{2n-1}$ increased as the equilibrium temperatures were lowered. At higher temperatures these materials appeared to

TABLE II

SHEAR PLANE SPACINGS FOR THE MEMBERS OF THE HOMOLOGOUS SERIES $\text{Cr}_2\text{Ti}_{n-2}\text{O}_{2n-1}$ WITH $\{121\}$ CS OBSERVED AFTER ANNEALING AT 1570 K

n	O:Me	D_{sp} ca:cd		D_{sp} obsd
6	1.833	0.929nm ^a		0.944 ^a
7	1.857	1.095 ^a	1.123nm ^b	1.118 ^a 1.10 ± 0.03nm ^c
8	1.875	1.266 ^a	1.292 ^b	1.286 ^a 1.30 ± 0.05 ^c
9	1.889	1.435 ^a	1.460 ^b	1.450 ^a 1.47 ± 0.02 ^c
10	1.900		1.629 ^b	1.59 ± 0.04 ^c
11	1.909		1.798 ^b	1.77 ± 0.02 ^c

^a Andersson et al. (15).

^b Calculated using the formula $D_{\text{sp}} = d_{121} (n - 0.347)$ (5).

^c This work.

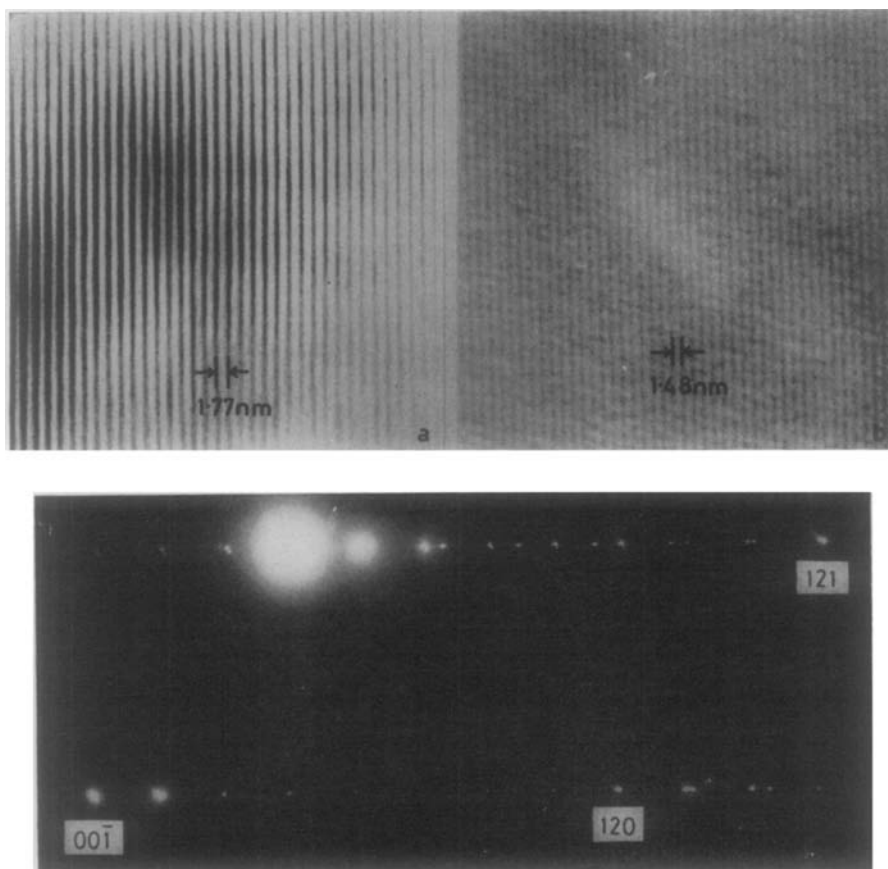


FIG. 8. (a), (b) Resolved, well-ordered CS planes corresponding to different compositions within the same sample. (c) Corresponding diffraction pattern, with sharp superlattice spots of two multiplicities.

form rutile solid solution without planar defects or ordered structures.

Between these two series is a range of intermediate compositions with a highly significant characteristic: the direction of superlattice ordering in any crystal sample appears to be oblique to, and to lie between, $\langle 121 \rangle$ and $\langle 132 \rangle$ and to vary with composition. This has not yet been completely elucidated, but certain features emerge clearly.

In all the structures that generate crystallographic shear phases, it has now been found that in different ranges of composition collapse takes place on two or more different $\{hkl\}$ planes—e.g. in $\text{Ti}_n\text{O}_{2n-1}$, in $\text{Mo}_n\text{O}_{3n-m}$, in the ReO_3 -based intermediate oxides of tungsten. Over a certain range of average composition there must be some mechanism for reorienting the CS planes. In principle, two distinct situations can be envisaged: (a) there is an essentially classical discontinuity, with two structures having different CS plane orientations and different compositions coexisting in separate crystals

or in intergrown domains, the one being progressively replaced by the other as the anion:cation ratio is altered; (b) the regularly recurrent boundaries between the slabs of parent structure are not constrained to one or other of the limiting low-index orientations, but may take up intermediate orientations. The essence of crystallographic shear is that some sheet of anion sites, with the orientation $(h_i k_i l_i)$, is eliminated from the crystal, the density of anion sites in that plane being s_i . If then we consider a column of crystal in a CS plane, extending along some particular direction—e.g. along $[100]$ of the rutile structure—such a column, N rutile cells in length, would intersect \mathcal{N}_i CS planes, and the nett anion:cation ratio would be $2 - (\mathcal{N}_i s_i / N)$. As long as the orientation of the CS planes remains constant, \mathcal{N}_i is the only variable, and changes of composition involve changes in the spatial separation of CS planes—i.e., changes in \mathcal{N}_i . This is the rationale of the homologous series of compounds. A suggestive common feature of the known CS

structure is that the changeover of CS plane orientation seems to take place in such a way that the lower limiting member of one homologous series and the uppermost member of the next have slabs of parent structure of much the same thickness: they differ in composition because the density of eliminated anion sites changes as the CS plane orientation is changed from $(h_1 k_1 l_1)$ to $(h_2 k_2 l_2)$. It may be tentatively postulated that the number of CS planes \mathcal{N}_i remains constant; s_i changes from s_1 to s_2 .

The question then arises whether the CS planes could pivot around to make s_i , $(h_i k_i l_i)$ continuously variable. The observed limiting CS plane orientations lie in the $\langle 1\bar{1}1 \rangle$ zone; the oblique superlattice directions that we have observed also lie in or close to this zone. If the crystallographic shear structures are drawn for other superlattice directions of not too high index, lying between $\langle 121 \rangle$ and $\langle 132 \rangle$, it may be seen (Fig. 9) that whilst the mean orientation changes progressively the columns of face-sharing octahedra strictly define a puckered boundary, with alternate segments of $\{121\}$ and $\{132\}$ structure, and that a continuous transformation should be possible. It would involve a sequence of changes in which lines of cation sites, lying along $\langle 1\bar{1}1 \rangle$ and adjacent to the shear plane, were sequentially displaced by $\sim \frac{1}{2}\langle 011 \rangle$, so that the location of the condensed groups of $[\text{TiO}_6]$ octahedra was progressively shifted. To establish order during such changes would require cooperative interactions, but the same mechanistic requirement is, in any case, involved in the creation, elimination and ordering of shear planes in any orientation. The intermediate orientation stages, with regularly puckered CS planes, are

of the kind envisaged by Spyridelis, Delavignette and Amelinckx (16) as giving rise to so-called orientation anomalies of superlattice spots. If the segments of the high-index CS planes showed variations in extent (giving bent CS plane boundaries in the extreme case), the diffraction patterns would show streaking transversely to the arrays of spots. These chromium-titanium oxides structures evidently achieve a high degree of regularity; neither the diffraction patterns nor the lattice images indicate any zig-zag shear planes at the microscope resolution attainable.

Not only the orientation, but also the spacing of the superlattice showed some variation: the distribution of observed spacings is shown in the histogram of Fig. 10 (a). Such a variation of spacing, at constant linear density of shear planes, is to be expected as the shear planes swing through the small angle from $\{121\}$ to $\{132\}$. Figure 10 (b) shows the relation between shear-plane spacing, orientation (angle $\langle 121 \rangle$ $\langle hkl \rangle$) and composition for homologous series based on a few rational shear plane directions, calculated using the same idealized collapse factor for all. Superimposed on this are observed values of D_{cs} corresponding to measured superlattice orientations. Because the arrays of superlattice spots are short, this angle can be measured only with low accuracy, so that each point has a substantial error disc. It is clear, however, that the varying superlattice spacings fall consistently along a path of changing composition, compatible with the hypothesis of pivoting shear planes.

A second finding of some significance is that, at low chromium concentrations, no extended defects

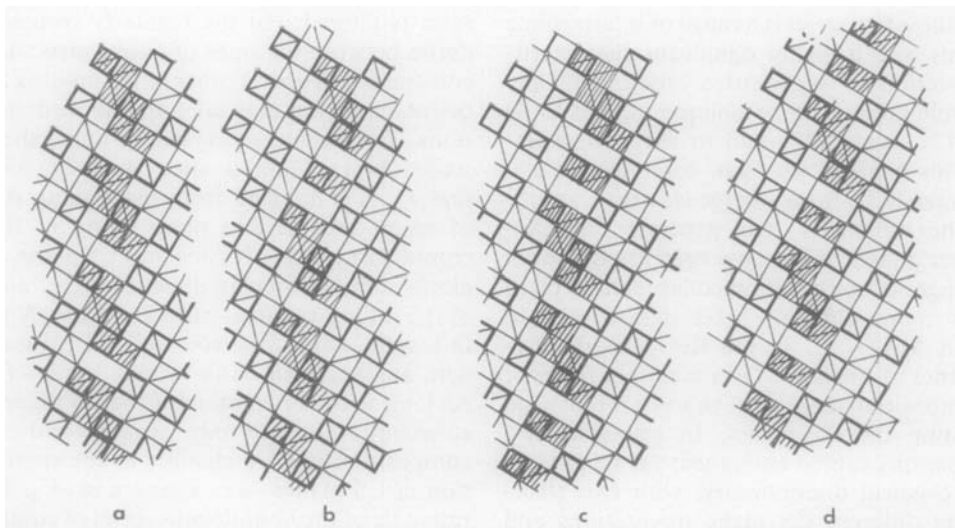


FIG. 9. Structure of CS planes, within the $[1\bar{1}1]$ zone, with orientations (a) $\{121\}$, (b) $\{374\}$, (c) $\{253\}$, (d) $\{132\}$.

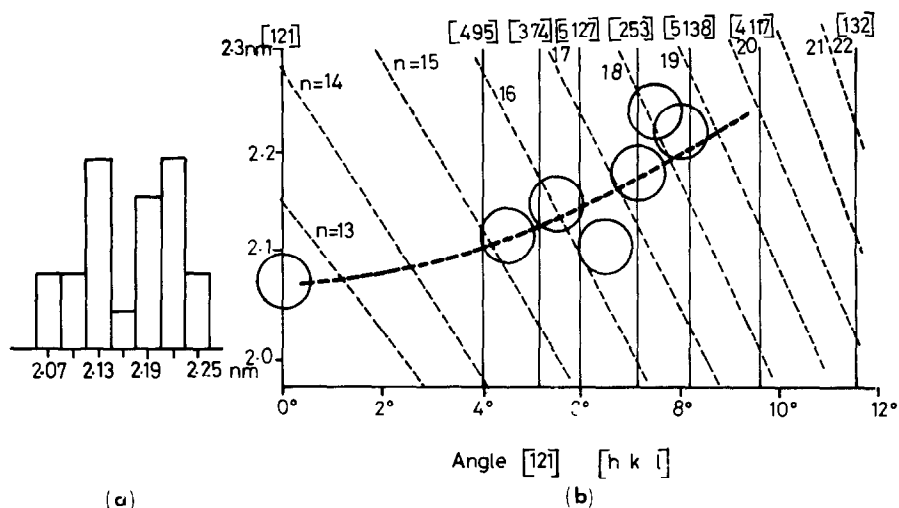


FIG. 10. (a) Histogram of observed CS spacings; (b) Dotted lines show the relation between CS plane spacing and composition (M_nO_{2n-1}), for CS plane orientations in the $[1\bar{1}1]$ zone, between $\{121\}$ and $\{132\}$. Circles indicate observed superlattice spacings and angle of superlattice direction to $[121]$, lying on a curve of continuous compositional change and orientation.

can be detected. The limiting composition of the apparently anion-deficient rutile structure extends to higher chromium concentrations at high temperatures, in accordance with the phase diagram of Flörke and Lee, and it appears to represent an equilibrium situation since domains of boundary-free rutile can coexist with lamellae of $\{132\}$ CS phase. In their work on the binary Ti-O system, Bursill and Hyde (10) found that in such ordered packets of CS plane structure, the spacing within a cluster was larger at the edge than at the centre. A smaller effect of this kind was observed here, a microdensitometer trace showing a change of spacing from 2.86 nm at the centre to about 3.2 nm between the outermost fringes. The observation that domains containing CS planes in two different orientations (Fig. 7) can exist within one crystal suggests an explanation of the twinning that has repeatedly been observed in these samples, and in reduced rutile. With eight possible $\{hkl\}$ orientations, the inception of crystallographic shear on two or more orientations is inherently likely. If the domains grow both by elongation and by addition of further slabs of shear structure, they will eventually grow together. The most energetically favourable interface between them will then be a twin-like boundary. If the two domains are identical in composition, a true twin would result; if they differ in composition, and hence in CS plane spacing, a coherent boundary terminating the CS planes can still be formed, across which the rutile parent structure, the subcell of the CS phases, is twinned. The probable con-

figuration of such boundaries on $\{100\}$ rutile can readily be drawn.

The real problem, however, is the defect structure of rutile with 0–5 mol % $\text{CrO}_{1.5}$. Whereas TiO_{2-x} appears unable to tolerate randomized defects, above the 10^{-4} concentration level at most (10), the chromium doped material accommodates a 2% deviation from stoichiometry without eliminating anion sites by crystallographic shear. Flörke and Lee discussed the possibility of incorporation as Cr^{4+} , but it is improbable that activity effects could bring about the necessary displacement of chemical potentials in the $\text{Cr}^{3+}/\text{Cr}^{4+}$ system. Indeed, the considerable amount of spectroscopic and ESR work on low-chromium-doped rutile, recorded in the literature, supports the view that chromium is present on normal lattice sites as Cr^{3+} . It is then inescapable that, up to a relatively high Cr^{3+} cation concentration, a nett anion deficiency is accommodated as randomized point defects or defect complexes. It is still unresolved whether vacant anion sites or interstitial cations would be the more-favoured defect type in the rutile structure. Flörke and Lee suggested that chromium would enter the octahedral interstitial sites, and that size effects and other interactions should lead to the clustering of chromium cations in such a way as to constitute a nucleus of the face-sharing $[\text{MO}_6]$ coordination octahedra of a shear plane. This may be so, but we have found no electron microscope evidence for the formation of interstitial discs, or of any form of clustering that would give localized

diffraction contrast effects detectable at the 0.5–0.7 nm scale of resolution. The present balance of evidence thus favours a point-defect description.

If this is so, conclusions drawn from work on doped oxides and ternary solid solutions must be extended only cautiously to binary mixed valence or nonstoichiometric systems. An important difference arises in respect of the more stringent requirements for ordering and the effect of self-diffusion processes in the ternary systems. Considerations of local electroneutrality (Pauling's rules) indicate that the cations of lower valence will be preferentially located in the shear planes. Crystallographic shear in the Cr–Ti oxides therefore presupposes a high degree of cooperative ordering, and the development of the superlattice structure could well be kinetically hindered. With Cr³⁺ as minor component, the requisite diffusion and ordering processes appear to be notably facile. However, not only kinetics but also equilibrium or steady-state configurations are involved. The occurrence of ordering at and above about 1200 K implies active self-diffusion. In the binary oxide, self-diffusion events lead only to an interchange of titanium atoms between CS plane sites and rutile slab sites without necessarily altering the spatial distribution of +3 and +4 cations; in the ternary oxides, a self diffusion event moving a chromium atom out of a CS plane site impairs the charge distribution and the perfection of order. The probability of such an occurrence depends upon a site-preference energy, and at high temperatures there will be some steady-state distribution of Cr³⁺ ions between the CS planes and the sites in the slabs of rutile structure. It is qualitatively understandable that, for low chromium concentrations, the requisite ordering of Cr³⁺ atoms over a sufficient area of a single {132} cationic sheet could not be sustained, so that the isolated crystallographic shear plane

became unstable with respect to dissociation into isolated defects.

Acknowledgments

The authors thank the U.K.A.E.A. for supporting this work and the Science Research Council.

References

1. A. D. WADSLEY, "Nonstoichiometric compounds," (L. Mandelcorn, Ed.), p. 98, Academic Press, New York, 1964.
2. S. ANDERSSON AND L. JAHNBERG, *Arkiv Kemi* **22**, 413 (1963).
3. S. ANDERSSON, B. COLLEN, U. KUYLENSTIERNA, AND A. MAGNELI, *Acta Chem. Scand.* **11**, 1641 (1957).
4. S. ANDERSSON, *Acta Chem. Scand.* **14**, 1161 (1960).
5. L. A. BURSILL, B. G. HYDE, O. TERASAKI, AND D. WATANABE, *Phil. Mag.* **20**, 347 (1969).
6. J. VAN LANDUYT AND S. AMELINCKX, *Mat. Res. Bull.* **5**, 267 (1970).
7. J. S. ANDERSON AND R. J. D. TILLEY, *J. Solid State Chem.* **2**, 472 (1970).
8. L. A. BURSILL AND B. G. HYDE, *Proc. Roy. Soc.* **A320**, 147 (1970).
9. L. A. BURSILL AND B. G. HYDE, *Acta Cryst.* **27**, 210 (1971).
10. L. A. BURSILL AND B. G. HYDE, *Phil. Mag.* **23**, 3 (1971).
11. O. TERASAKI AND D. WATANABE, *Jap. J. Appl. Phys.* **10**, 292 (1971).
12. O. W. FLÖRKE AND C. W. LEE, *J. Solid State Chem.* **1**, 445 (1970).
13. P. B. HIRSCH, A. HOWIE, R. B. NICHOLSON, D. W. PASHLEY, AND M. J. WHELAN, "Electron Microscopy of Thin Crystals," Butterworths, London, 1965.
14. J. S. ANDERSON AND B. G. HYDE, *J. Phys. Chem. Sol.* **23**, 1393 (1967).
15. S. ANDERSSON, A. SUNDHOLM, AND A. MAGNELI, *Acta Chem. Scand.* **13**, 989 (1959).
16. J. SPYRIDELIS, P. DELAVIGNETTE, AND S. AMELINCKX, *Phys. Status. Solidi* **19**, 683 (1967).